ELSEVIER

Polymer 42 (2001) 3205–3211

polymer

www.elsevier.nl/locate/polymer

# Effect of chain architecture of graft copolymer on the structure of adsorbed layer: a Monte Carlo simulation approach

K.H. Kim, W.H. Jo*

*Hyperstructured Organic Materials Research Center and Department of Fiber and Polymer Science, Seoul National University, Seoul 151-742, South Korea*

Received 13 December 1999; received in revised form 6 July 2000; accepted 30 August 2000

**Abstract**

The effect of chain architecture of graft copolymer on the structure of an adsorbed layer on a surface is investigated using an off-lattice Monte Carlo simulation method. The graft copolymers used for the simulation have the same composition but different chain architecture. The simulation results show that the layer thickness of multi-chains adsorbed onto the surface first decreases with increasing the number of side chains, indicating that the chain conformation of the adsorbed polymer becomes more flattened as the length of the side chain becomes shorter. When the length of the side chain decreases further than a critical length, however, a slight increase in layer thickness is observed, accompanied with an increase in the population of loosely bound chains. 

*Keywords*: Adsorption; Graft copolymer; Monte Carlo simulation

## 1. Introduction

The conformation of a polymer adsorbed on a surface, which may be different from that in the bulk state, is described in terms of various parameters such as the adsorbed amount, surface coverage, layer thickness, and average bound fraction of polymer segments [1–33]. These parameters depend strongly on the properties of the systems such as the length of adsorbing and non-adsorbing blocks, the bulk volume fraction, the adsorption energy parameters, and the solvent–polymer interaction parameters.

There have been a number of theoretical [3–6], experimental [2,7–14], and computer simulation [15–31] studies on the structure of the adsorbed layers for various polymers such as homopolymers [15–18], diblock copolymers [19–21], triblock copolymers [22–24], random or alternating copolymers [25–27], and end-functionalized polymers [28].

The adsorption of diblock copolymer from both selective and non-selective solvents has been investigated using a variety of experimental methods [2]. For instance, Belder et al. [9] studied the adsorption behavior of poly(styrene-*b*-2-vinylpyridine) block copolymers with a fixed length of the non-sticky styrene block but with different lengths of the sticky 2-vinylpyridine block. Their experimental results show that the layer thickness remains almost constant irrespective of the sticky block length. The adsorption behavior of branched polymers onto the metal surface has been experimentally studied by Kawaguchi and Takahashi [14]. Their results show that the adsorption of comb-branched polystyrene is larger than that of linear polystyrene with the same molecular mass, while the chain extension of the branched one at the adsorbed layer is smaller than the linear one, reflecting that the segment density of the branched polystyrene at the polymer–metal interface is higher than the linear polystyrene. Although several other experiments have been done on the adsorption behavior of various polymers, the microscopic explanation on the adsorption is still lacking.

Computer simulations have many advantages over experiments in gaining insight into the behavior of the adsorbed layer at the molecular level. Furthermore, the effect of chain architecture can easily be taken into account by computer simulation. Mattice and coworkers [20,21] simulated the adsorption behavior of diblock copolymers in a selective solvent as functions of adsorption energy, volume fraction and block size. They found that the bound fraction of the sticky block decreased with increasing the length of the sticky block. Balazs et al. [27,30] examined the effect of the sequence of monomers in a copolymer on the structure of the adsorbed layer. They found that the structure of the adsorbed layer was sensitive not only to the amount of sticky segments in the chain but also to the sequence of the units along the chain.

* Corresponding author. Tel.: +82-2-880-7192; fax: +82-2-885-1748.
*E-mail address:* whjpoly@plaza.snu.ac.kr (W.H. Jo).

0032-3861/01/$ - see front matter 
PII: S0032-3861(00)00728-X

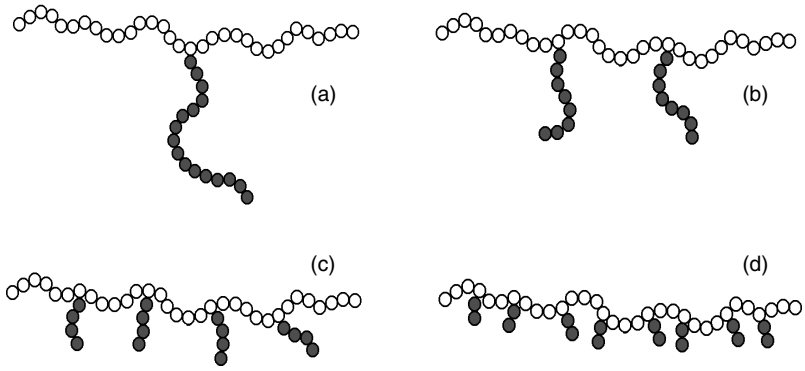


Fig. 1. Schematic structure of graft copolymers used for simulation: (a) B32G16 − 1; (b) B32G8 − 2; (c) B32G4 − 4; (d) B32G2 − 8.

Although much effort has been devoted to clarifying the properties of the adsorbed layer formed by polymers with various chain structures, few studies have been focused on the adsorption of graft copolymers. In this paper, the chain architecture of graft copolymers is systematically varied, and the effect of chain architecture on the adsorption of graft copolymers onto a solid surface was investigated using an off-lattice Monte Carlo simulation technique.

## 2. Model and simulation

An off-lattice Monte Carlo model used for this study is only briefly described here because more details are found elsewhere [33–35,36–38]. Each coarse-grained bond is described by the finitely extensible non-linear elastic (FENE) potential for a bond length $l$ which is restricted to the interval $l_{\min} < l < l_{\max}$

$$U_{\mathrm{FENE}}(l) = -K(l_{\max} - l_0)^2 \ln\left[1 - \left(\frac{l - l_0}{l_{\max} - l_0}\right)^2\right], \qquad (1)$$

$$l_0 = \frac{l_{\min} + l_{\max}}{2}, \qquad (2)$$

$$U_{\mathrm{FENE}}(l \le l_{\min}) = U_{\mathrm{FENE}}(l \ge l_{\max}) = \infty.$$

Obviously the minimum of this potential occurs at $l = l_0$, and the potential is harmonic near $l_0$. The spring constant $K$ (in units of $kT$) controls the width of the potential near the minimum. The parameters of the FENE potential are set to $K/k_{\mathrm{B}}T = 20$, $l_{\min} = 0.4$ and $l_{\max} = 1$, yielding $l_0 = 0.7$. The non-bonded interaction between effective monomers is described by a Morse-type potential:

$$U_{\mathrm{M}}(r)/\varepsilon_{\mathrm{M}} = \exp[-2\alpha(r - r_{\min})] - 2\exp[-\alpha(r - r_{\min})], \qquad (3)$$

where $r$ is the distance between the beads representing the effective monomeric units, $r_{\min}$ denotes the distance at the minimum of the potentials, and $\varepsilon_{\mathrm{M}}$ (in units of $kT$) determines the depth of the minimum. Morse parameters are chosen as $\varepsilon_{\mathrm{M}}/k_{\mathrm{B}}T = 0.1$, $\alpha = 24$, and $r_{\min} = 0.8$ throughout all simulations. At given values of the $k_{\mathrm{B}} = 1$ and $\varepsilon_{\mathrm{M}} = 0.1$, the $\theta$ temperature is approximately equal to 0.62 [36]. Thus, the temperature $T = 1$ used in this simulation implies $T \gg \theta$ (good solvent conditions). Also, the advantage of this choice is that the decay of the Morse-type potential with the distance $r$ is so rapid that $U_{\mathrm{M}}(r) \approx 0$ for $r > 1$ with negligible error. This allows us to use a link-cell algorithm with the cell linear dimension of unity [34].

The backbone of the graft copolymer is composed of 32 segments, and the side chains grafted onto the backbone are separated by an equal spacer length. The side chain length of graft copolymer is varied from 2 to 16. Since the total number of side chain segments per copolymer is kept constant as 16, the number of grafted side chains is varied from 8 to 1. The backbone is composed entirely of non-sticky units, while the side chains are made up of sticky units. Consequently, all graft copolymers for simulation have the same number of sticky side units but with different chain architectures. All the chain architectures used in this study are schematically drawn in Fig. 1 and summarized in Table 1. The notation for these model graft copolymers is given as follows: B(the number of backbone

Table 1
Structure of graft copolymers used for simulation

| Designation | Length of backbone chain | Length of side chain | Number of side chains |
|---|---|---|---|
| B32G16–1 | 32 | 16 | 1 |
| B32G8–2 | 32 | 8 | 2 |
| B32G4–4 | 32 | 4 | 4 |
| B32G2–8 | 32 | 2 | 8 |
| B32G1–16 | 32 | 1 | 16 |

segments)G(the number of side chain segments) − (the number of side chains), e.g. the notation B32G8 − 2 means that the length of backbone chain is 32 and the length and number of grafting chain are 8 and 2, respectively.

Simulation was performed on a $L = 32 \times 32 \times 32$ cubic cell with periodic boundary conditions in $x$ and $y$ directions. For adsorption, the attractive wall and impenetrable wall were placed at $z = 0$ and $z = L$, respectively. When a sticky side chain segment of graft copolymer is placed near the wall, the attractive square well potential is used:

$$U_W(z) = \varepsilon,\ z \le \delta_z;\ \ U_W(z) = 0,\ z > \delta_z, \tag{4}$$

where $\delta_z = 1/8$.

This type of potential has been used by Milchev and Binder [36,37] and proved to be physically reasonable, since each effective bond represents a sequence of several chemical monomers. To investigate the effect of this attractive potential ($\varepsilon/k_BT$) on graft copolymer adsorption, simulations are carried out over a wide range of the strength of this attractive potential from weakly attractive ($\varepsilon/k_BT \approx \varepsilon_c/k_BT = -1.90 \pm 0.05$ [37]) to strongly attractive condition ($\varepsilon/k_BT = -5.00$). Here we used only one interaction parameter between segments, $\varepsilon_M$ ($= \varepsilon_{BB} = \varepsilon_{BG} = \varepsilon_{GG} = 0.1kT$, where the subscripts B and G denote backbone and graft chain, respectively), since we are only interested in the effect of attractive potential $\varepsilon$ between the graft segment and the wall on the adsorption behavior. With these interaction parameters, we can more easily focus on the adsorption behavior itself without facing any other undesirable effects such as chain aggregation in solution.

Initially, 29 chains are placed randomly in the simulation box so that the number density becomes $\phi \approx 0.043$, which can be regarded as a dilute solution [31,33]. When one chain is bound to the surface, a new chain is added into the system at a random position, and when a chain is desorbed from the surface, the chain farthest from the wall is removed from the system. In this way, the number of free chains in the bulk solution is held constant throughout the simulation. This means that the system is in contact with a solution reservoir that supplies chains to the wall without limit. In other words, our simulation uses the grand canonical ensemble: the number of chains in solution is not constant, but fluctuates continually. This prevents depletion of the bulk solution and the gradual decay of its osmotic pressure [16,27,28,30]. For the case of single chain adsorption, the above ensemble was not used, i.e. only one chain is inserted into the bulk solution and adsorbed on the wall surface. The single chain adsorption is compared with multi-chains adsorption.

In order to equilibrate an initial state, the system was relaxed for a long time in the absence of adsorption potential. Then, simulations are implemented for over one million MCSs until the surface has effectively been saturated and thus the surface coverage reaches an equilibrium value. All the properties reported here are the values averaged over the last one million MCSs. As the time unit, a Monte Carlo step (MCS) is defined as one attempted trial per segment to move on the average.

## 3. Results and discussion

Fig. 2 shows the change of the number of adsorbed chains and the surface coverage (the number of adsorbed segments per unit volume at the surface defined as $L_x \times L_y \times \delta_z$) with simulation time for various chain architectures. The general shape of the curves shows an agreement with experimental observations [12]: the number of adsorbed chains and the surface coverage gradually level off as the time approaches one million steps, indicating that the surface becomes saturated.

Before we analyze the change in chain conformation of graft copolymers when adsorbed on the solid surface, we first determine the structure of the free graft copolymer chains not in contact with the solid surface. Table 2 shows the root mean square radius of gyration ($\langle Rg^2\rangle^{1/2}$) and the root mean square chain end-to-end distance of the backbone ($\langle r_e^2\rangle_b^{1/2}$) for each free graft copolymer. As the chain architecture changes from B32G16 − 1 to B32G1 − 16, the end-to-end distance of the backbone chain slightly increases, i.e. the backbone stretches with decreasing the number of grafted side chains. This somewhat stretched structure will have an effect on adsorption dynamics and

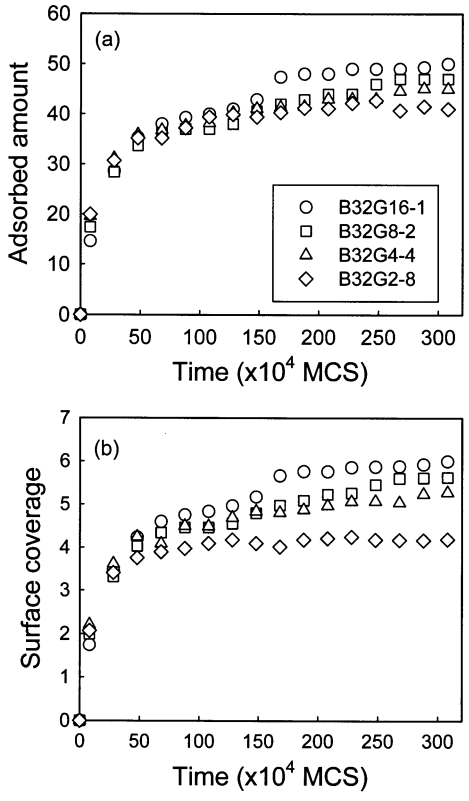


Fig. 2. Plots of (a) adsorbed amount and (b) surface coverage versus time (MCS) for various chain architectures at $\varepsilon = -5kT$.

Table 2
Chain dimensions for free graft copolymer in solution

| Copolymers | $\langle Rg^2\rangle^{1/2}$ | $\langle r_e^2\rangle_b^{1/2}$ |
|---|---|---|
| B32G16–1 | 2.36 ± 0.05 | 5.36 ± 0.32 |
| B32G8–2 | 2.33 ± 0.08 | 5.64 ± 0.38 |
| B32G4–4 | 2.32 ± 0.07 | 5.78 ± 0.36 |
| B32G2–8 | 2.44 ± 0.07 | 6.14 ± 0.35 |
| B32G1–16 | 2.71 ± 0.15 | 6.73 ± 0.51 |

bound layer properties of graft copolymers that will be discussed later.

The adsorption of a single chain with various chain architectures is simulated at $\varepsilon = -5kT$ before discussing the adsorption behavior of multi-chains systems. As the chain architecture changes from B32G16 − 1 to B32G1 − 16, the bound fraction of the side chain segments ($f_s$) decreases, whereas the center of mass in the $z$ direction ($CM_z$) for a single bound chain shows a minimum, as can be seen in Table 3. In other words, the chain becomes flattened first and then becomes more stretched normal to the surface as the chain architecture changes from B32G16 − 1 to B32G1 − 16, as also verified by the values of $(\langle Rg_z^2\rangle/\langle Rg_{xy}^2\rangle)^{1/2}$ in Table 3. A more stretched structure normal to the surface, which is seen in this single chain case, is not observed in the multi-chains case. These representative chain structures are visualized in Fig. 3, when each single chain is adsorbed onto the solid surface.

The bound layer properties of graft copolymer chains are summarized in Table 4, when multi-chains were adsorbed onto the solid surface at $\varepsilon/k_BT = -5$, where the values of $k_B$ and $T$ are given unity in our simulation so that the unit of energy ($kT$) is omitted afterwards. The bound layer properties at $\varepsilon = -4$, $\varepsilon = -3$ and $\varepsilon = -2$ also showed the same behavior as the case of $\varepsilon = -5$ (not shown here). The number of bound chains decreases with increasing the

Table 3
Properties of a single chain bound to the surface when simulated under the condition of $\varepsilon = -5kT$

| Copolymers | $f_s$[a] | $CM_z$[b] | $\langle Rg_z^2\rangle^{1/2}$ | $\langle Rg_{xy}^2\rangle^{1/2}$[c] | $\langle r_e^2\rangle^{1/2}$ | $(\langle Rg_z^2\rangle/\langle Rg_{xy}^2\rangle)^{1/2}$ |
|---|---|---|---|---|---|---|
| B32G16–1 | 0.96 ± 0.05 | 1.53 ± 0.37 | 1.41 ± 0.36 | 1.95 ± 0.36 | 6.20 ± 2.18 | 0.72 |
| B32G8–2 | 0.94 ± 0.10 | 1.17 ± 0.33 | 1.06 ± 0.28 | 1.91 ± 0.31 | 6.33 ± 2.33 | 0.55 |
| B32G4–4 | 0.88 ± 0.18 | 0.98 ± 0.45 | 0.82 ± 0.31 | 1.93 ± 0.48 | 6.92 ± 2.71 | 0.42 |
| B32G2–8 | 0.48 ± 0.29 | 2.32 ± 1.48 | 1.65 ± 0.94 | 1.69 ± 0.42 | 7.27 ± 2.40 | 0.98 |
| B32G1–16 | 0.14 ± 0.11 | 4.04 ± 1.41 | 2.37 ± 0.83 | 1.57 ± 0.45 | 8.59 ± 2.20 | 1.52 |

[a] Fraction of side chain segments bound to the surface.
[b] Center of mass along the $z$-axis averaged for several runs.
[c] Radius of gyration in $x$, $y$ directions averaged for several runs $((\langle Rg_x^2\rangle^{1/2} + \langle Rg_y^2\rangle^{1/2})/2)$.

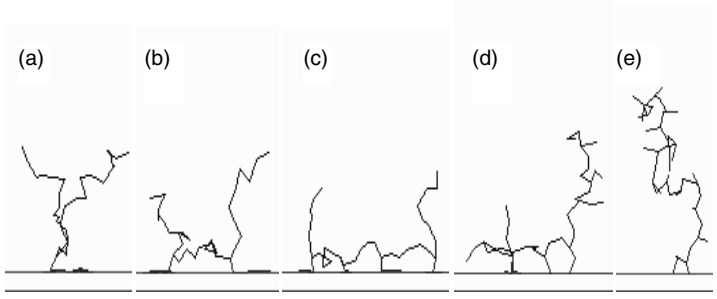


Fig. 3. Snapshot pictures of a single chain adsorbed on the surface at $\varepsilon = -5kT$ : (a) B32G16 − 1; (b) B32G8 − 2; (c) B32G4 − 4; (d) B32G2 − 8; (e) B32G1 − 16.

Table 4
Properties of the bound layer when multi-chains are adsorbed at $\varepsilon = -5kT$

| Copolymers | $f_s$ | Number of bound chains | Surface coverage[a] | $\langle z\rangle_{high}$ | $CM_z$ |
|---|---|---|---|---|---|
| B32G16–1 | 0.96 ± 0.01 | 49.04 ± 0.77 | 5.88 ± 0.10 | 5.28 ± 0.15 | 1.85 ± 0.05 |
| B32G8–2 | 0.95 ± 0.01 | 45.51 ± 1.79 | 5.43 ± 0.23 | 4.26 ± 0.14 | 1.38 ± 0.04 |
| B32G4–4 | 0.91 ± 0.02 | 43.79 ± 1.49 | 5.09 ± 0.16 | 3.36 ± 0.14 | 1.04 ± 0.06 |
| B32G2–8 | 0.77 ± 0.02 | 41.71 ± 1.30 | 4.18 ± 0.11 | 3.18 ± 0.19 | 1.04 ± 0.08 |
| B32G1–16 | 0.64 ± 0.09 | 32.10 ± 2.32 | 2.83 ± 0.31 | 3.12 ± 0.50 | 1.12 ± 0.20 |

[a] Number of segments per the layer volume defined as $N_x \times N_y \times \delta$ where $\delta$ is 1/8.

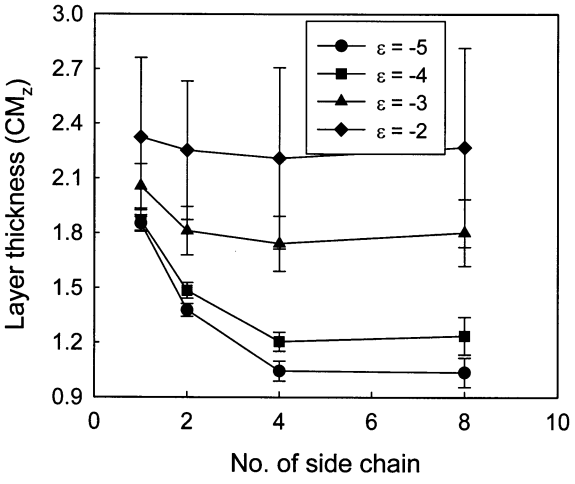


Fig. 4. Plots of the layer thickness measured by the center of mass along the $z$-axis versus the number of side chains, under various adsorption potentials.

number of grafted side chains, i.e. as the chain architecture changes from B32G16 − 1 to B32G2 − 8. The bound fraction of the side chain segments, which provides a measure of the adhesion between the polymer and the substrate, shows the same tendency as the number of bound chains. The layer thickness may be represented by the average center of mass of each bound chain defined as:

$$\mathrm{CM}_z = \frac{1}{M}\sum_{i=1}^{M}\mathrm{CM}_{z,i}, \tag{5}$$

where $M$ is the number of bound chains and $\mathrm{CM}_{z,i}$ the center of mass of the $i$th bound chain. When the layer thickness represented by $\mathrm{CM}_z$ is plotted against the number of side chains in the copolymer under various adsorption potentials, it is clear that the layer thickness steeply decreases with increasing the number of side chains from 1 to 4 and then levels off, as shown in Fig. 4. This behavior becomes more obvious when the adsorption potential is large.

The distribution of both the backbone and the side chain segments in the $z$-direction from the surface is monitored in order to more specifically examine the structure of the bound layer. Fig. 5 compares the distribution of B32G16 − 1 with that of B32G2 − 8, when polymers are adsorbed at $\varepsilon = -5$. It is clear that the maximum $z$-coordinates of the backbone and the side chains for B32G2 − 8 are smaller than those for B32G16 − 1, indicating that the layer thickness of B32G2 − 8 is smaller than that of B32G16 − 1. Here it is noteworthy that the segment distribution of the side chains for B32G2 − 8 (Fig. 5b) shows two peaks with a weaker peak at $z = 4$. This indicates that some of the sticky side chains are not completely adsorbed onto the surface, i.e.

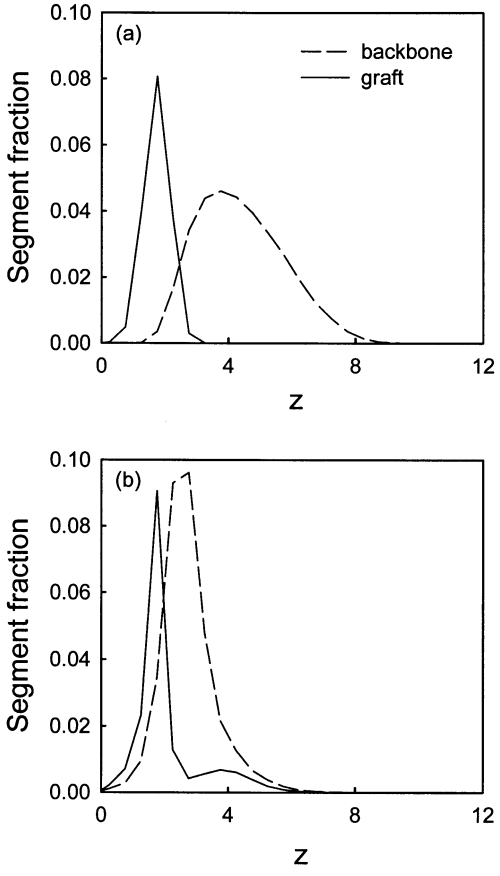


Fig. 5. Segment density distribution along the $z$-axis at $\varepsilon = -5kT$ for: (a) B32G16 − 1; (b) B32G2 − 8.

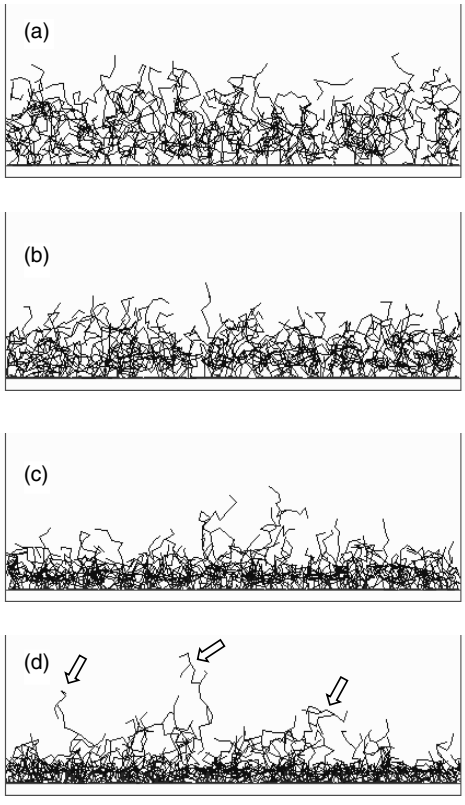


Fig. 6. Snapshot pictures showing the structure of bound layer when multi-chains are adsorbed onto the surface under the adsorption potential of $\varepsilon = -5kT$ for: (a) B32G16 − 1; (b) B32G8 − 2; (c) B32G4 − 4; (d) B32G2 − 8. The arrows in this figure indicate loosely bound chains.

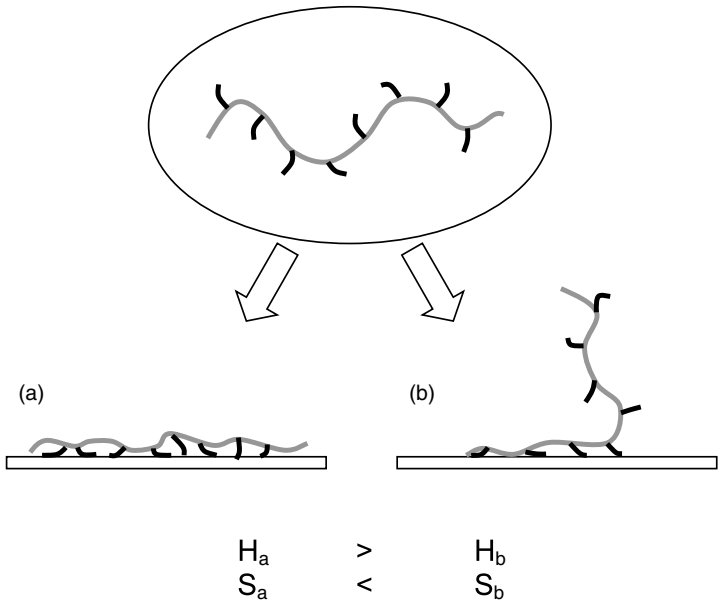


Fig. 7. Schematic representation of two possible chain conformations for B32G2 − 8: (a) enthalpically stabilized structure through attractive chain–surface contact; (b) entropically favorable structure occupying less space.

they are partially adsorbed onto the solid surface. In order to visualize this behavior, snapshot pictures are taken from samples simulated at $\varepsilon = -5$, as shown in Fig. 6. As can be seen in Fig. 6d, it is found that some of the B32G2 − 8 chains are loosely bound to the surface. This suggests that even under strongly attractive conditions, not all the side chains are adsorbed onto the surface, but some graft copolymers with short side chains are loosely bound to the surface and thus the chains are extended into the solution (see Fig. 6d). These loosely bound chains are primarily responsible for the weaker peak at $z = 4$ in Fig. 5b.

Graft copolymers with many short side chains under strongly attractive conditions can have energetically favorable chain conformations, as shown in Fig. 7a. But this enthalpic stabilization through the chain–surface contact is accompanied with entropic loss from polymer collapse and chain flattening. Furthermore, the enthalpically favorable chain conformation occupies more surface area. Therefore, when the surface becomes sufficiently crowded, both the excluded volume effect exerted by neighboring chains and the entropic gain effect due to chain recoiling compete with the enthalpic stabilization, as depicted in Fig. 7, and consequently the layer thickness does not decrease any further. Under weakly attractive conditions, the layer thickness rather increases slightly as the chain architecture changes from B32G4 − 4 to B32G2 − 8, because the enthalpic attraction energy is not enough to override entropic gain due to chain recoiling. These results suggest that there are a critical number of side chains at which the layer thickness shows a minimum under a specific attraction.

The development of loosely bound chains for B32G2 − 8 is verified in Fig. 8, which depicts the change of the segment fraction profile of the side chain for B32G2 − 8 at $\varepsilon = -5$ as a function of time. As the time lapses, the second density maximum for the side chains is developed (the first peak is cut off for clarity), which means that the loosely bound chains are formed in the later stage as the surface is saturated with many late comers.

## 4. Conclusions

The effects of chain architecture of graft copolymer on the structure of an adsorbed layer are investigated using an off-lattice Monte Carlo simulation method. For adsorption

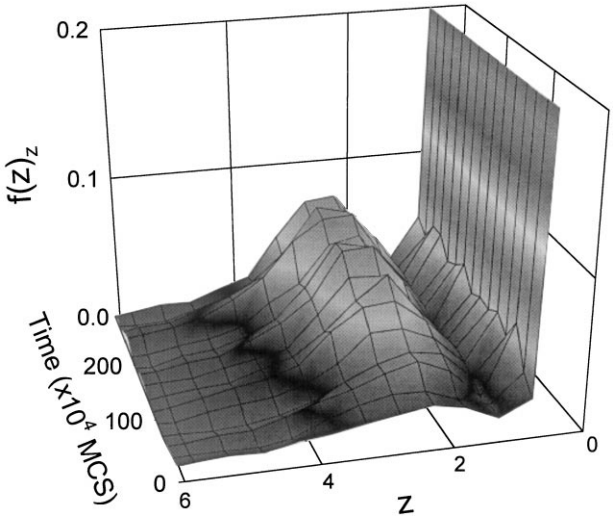


Fig. 8. Time evolution of the segment density distribution of side chain for B32G2 − 8 at $\varepsilon = -5kT$.

of a single chain, the chain conformation of an adsorbed polymer first becomes more flattened as the length of the side chain becomes shorter. But, as the length of the side chain decreases further, the chain conformation becomes more stretched normal to the surface accompanied with a decrease in the bound fraction. For multi-chains systems, the number of bound chains, the fraction of side chain segments bound to the surface, the surface coverage, and the average layer thickness decrease with increasing the number of side chains or with decreasing the length of the side chain, indicating that the chain conformation at the surface becomes more flattened as the length of the side chain becomes shorter. However, as the number of side chains exceeds a critical value (four in our simulation), some of grafted copolymer chains are partially adsorbed onto the adsorbed layer, which results in a slight increase in the layer thickness. These results can provide a guideline for designing the structure of graft copolymer for adsorption.

## References


[1] Sanchez IC. Physics of polymer surfaces and interfaces. Boston: Butterworths–Heinemann, 1992 (chap. 4).
[2] Cohen-Stuart M, Cosgrove T, Vincent B. Adv Colloid Interface Sci 1986;24:143.
[3] Scheutjens JMHM, Fleer GJ. J Phys Chem 1979;83:1619.
[4] Scheutjens JMHM, Fleer GJ. J Phys Chem 1980;84:178.
[5] de Gennes PG. Macromolecules 1980;13:1069.
[6] Kosmas MK. Macromolecules 1990;23:2061.
[7] Cosgrove T. J Chem Soc, Faraday Trans 1990;86:1323.
[8] Tassin JF, Siemens RL, Tang WT, Hadziioannou G, Swalen JD, Smith BA. J Phys Chem 1989;93:2106.
[9] Belder GF, ten Brinke G, Hadziioannou G. Langmuir 1997;13:4102.
[10] Guzonas DA, Boils D, Tripp P, Hair ML. Macromolecules 1992;25:2434.
[11] Wu DT, Yokoyama A, Setterquist RL. Polym J 1991;23:709.
[12] Xie M, Blum FD. Langmuir 1996;12:5669.
[13] Takahashi A. Polym J 1991;23:715.
[14] Kawaguchi M, Takahashi A. J Polym Sci, Polym Phys Ed 1980;18:943.
[15] Konstadinidis K, Prager S, Tirrell M. J Chem Phys 1992;97:7777.
[16] Zajac R, Chakrabarti A. J Chem Phys 1996;104:2418.
[17] King SM, Cosgrove T. Macromolecules 1993;26:5414.
[18] Shaffer JS. Macromolecules 1994;27:2987.
[19] Clancy TC, Webber SE. Macromolecules 1993;26:628.
[20] Zhan Y, Mattice WL, Napper DH. J Chem Phys 1993;98:7502.
[21] Zhan Y, Mattice WL, Napper DH. J Chem Phys 1993;98:7508.
[22] Balazs AC, Lewandowski S. Macromolecules 1990;23:839.
[23] Haliloglu T, Mattice WL. Macromol Theory Simul 1997;4:667.
[24] Haliloglu T, Stevenson DC, Mattice WL. J Chem Phys 1997;106:3365.
[25] Shaffer JS. Macromolecules 1995;28:7447.
[26] Zheligovskaya EA, Khalatur PG, Khokhlov AR. J Chem Phys 1997;106:8598.
[27] Balazs AC, Gempe M, Lantman CW. Macromolecules 1991;24:168.
[28] Zajac R, Chakrabarti A. Phys Rev E 1994;49:3069.
[29] Yethiraj A, Hall CK. Macromolecules 1991;24:709.
[30] Balazs AC, Siemasko CP. J Chem Phys 1991;95:3798.
[31] Rouault Y. Macromol Theory Simul 1998;7:359.
[32] Binder K. Monte Carlo and molecular dynamics simulations in polymer science. Oxford: Oxford University Press, 1995.
[33] Milchev A, Paul W, Binder K. J Chem Phys 1993;99:4786.
[34] Gerroff I, Milchev A, Binder K, Paul W. J Chem Phys 1993;98:6526.
[35] Olaj OF, Petrik T, Zifferer G. J Chem Phys 1997;107:10 214.
[36] Milchev A, Binder K. Macromol Theory Simul 1994;3:915.
[37] Milchev A, Binder K. Macromolecules 1996;29:343.
[38] Milchev A, Binder K. J Chem Phys 1997;106:1978.